Evaluation of Esophageal Cancers Using Fluorine-18-Fluorodeoxyglucose PET

Toru Fukunaga, Shinichi Okazumi, Yoshio Koide, Kaichi Isono and Keiko Imazeki

Second Department of Surgery and Department of Radiology, Chiba University School of Medicine, Chiba, Japan

To evaluate glucose metabolism in esophageal cancer, 48 patients were studied using PET with ^{18}F-2-fluoro-2-deoxy-D-glucose (FDG). **Methods:** After transmission scans were obtained, ^{18}F-FDG (148 MBq) was administered intravenously. In 11 patients, a dynamic study was performed to evaluate glucose metabolism. Using the changes of radioactivity in both plasma and tumor, rate constants (k1-k4) defined in the metabolic model for ^{18}F-FDG were calculated. In 48 patients, static PET scans of the tumor (5-min scans) were obtained 60 min after administration. Fluorine-18-FDG activity within each tumor was corrected for physical decay and normalized by dose administration and patient weight to produce a standardized uptake value (SUV). **Results:** Both the k3 value (n = 11) reflecting hexokinase activity and SUV (n = 13) were well correlated with hexokinase activity from the resected specimen (p < 0.05). Forty-seven of 48 patients before treatment revealed SUV greater than 2.0, but 10 normal control subjects and 1 esophageal benign tumor revealed less than 2.0 (accuracy rate 98.3%). Although clinicopathological findings did not correlate with SUV, except for two patients with carcinosarcoma, 23 patients with an SUV greater than 7.0 had a poor prognosis compared with 25 patients with SUVs less than 7.0. **Conclusion:** These findings suggest that ^{18}F-FDG PET may be useful in distinguishing malignant tumors from benign lesions and in the preoperative evaluation of the prognostic factor.

Key Words: PET; fluorine-18-fluorodeoxyglucose; esophageal cancer; prognosis

J Nucl Med 1998; 39:1002–1007

Esophageal cancer has one of the most unfavorable prognoses in digestive malignancies due to its biological behavior and surgical difficulties. Elucidation of the prognostic factor on the basis of biological viability of the tumor is essential in improving the prognosis of esophageal cancer. The rate of glucose metabolism is considered to increase in malignant tumors and correlates with tumor proliferative activity (*1,2*). In this study, for the purpose of evaluating glucose metabolism of esophageal cancer, ^{18}F-2-fluoro-2-deoxy-D-glucose (FDG) was used as a tracer for glucose metabolism, and PET was performed in patients with esophageal cancer. Fluorine-18-FDG PET has been used for various neoplasms (*3–6*), however, no detailed analysis of glucose metabolism in esophageal cancer has been revealed (*7*). We attempted to define a convenient and reliable index for clinical assessment of esophageal cancer and to predict prognosis before surgery.

MATERIALS AND METHODS

Patients

Between August 1988 and December 1995, 48 patients (43 men, 5 women; mean age 61.4 yr; age range 44–76 yr) with primary esophageal cancer underwent PET using ^{18}F-FDG before radical resection. All patients were untreated and selected based on tumor size, which was greater than 3 cm in diameter due to the limited

resolution of PET. All operations were performed by the same surgical team and all patients underwent clinical follow-up for a period of 2 mo to 7 yr after surgery. Postoperative recurrences were mainly diagnosed by conventional examinations (CT, ultrasound, radiography and others). Ten patients with a normal esophagus and one with benign esophageal tumor (granular cell tumor) were also studied as controls.

Tracer Synthesis and PET Scanning

Fluorine-18-FDG was synthesized by the acetylhypofluorite method with a CUPID automatic tracer synthesizer from ^{18}F manufactured with a small CYPRIS cyclotron (Sumitomo Heavy Industries, Tokyo, Japan). PET images were obtained on a HEAD-TOME III (Shimazu Works, Kyoto, Japan) scanner. A ramp filter and a Butterworth filter (cutoff frequency: 8 mm^{-1}, order 3) were used for image reconstruction, resulting in an in-plane spatial resolution of 10.5 mm (FWHM) with z-axis resolution of 16.5 mm (*6*).

After transmission scanning with a ^{68}Ge ring, ^{18}F-FDG (148 MBq) was administered intravenously. PET scanning of the tumor (5 min scans) was initiated 60 min after administration. Fluorine-18-FDG activity within each tumor was corrected for physical decay and normalized by dose administration and patient weight to produce a standardized uptake value (SUV) (*8*). Mean radioactivity (cps/ml) value was determined at the designated site of maximum accumulation (9 pixels; 9 × 9 mm^2 in the tumor. No correction for the tumor-to-blood volume was made.

A dynamic study for detailed evaluation of glucose metabolism were performed in 11 patients for a fixed duration (from February 1990 to September 1991). Arterial blood samples were collected from the brachial artery (nine 15-sec interval, four 30-sec interval, four 1-min interval, two 2-min interval, one 3-min interval, three 5-min interval and three 10-min interval), and dynamic scans of the tumor were performed (five 2-min scans and ten 5-min scans). Changes in radioactivity of plasma (Cp) were measured with a well counter and radioactivity changes in tumor (Ci) were evaluated through PET images. Rate constants defined by Phelps et al. (*9*) in a metabolic model for ^{18}F-FDG in brain tissue (Fig. 1) were calculated by a nonlinear least squares method (*6*). The rate constants used were: k1 = transfer from blood into tissue; k2 = transfer from tissue into blood; k3, = phosphorylation by hexokinase; k4 = dephophorylation by glucose-6-phosphatase.

Measurement of Tumor Hexokinase Activity

Hexokinase activities of the resected tumor tissues were simultaneously measured in accordance with the method of Monakhov et al. (*10*) in 13 patients (11 of whom underwent a dynamic study). The tissue specimens for analysis were obtained immediately after resection from the area corresponding to the region of interest in the preoperative PET images with reference to other image findings.
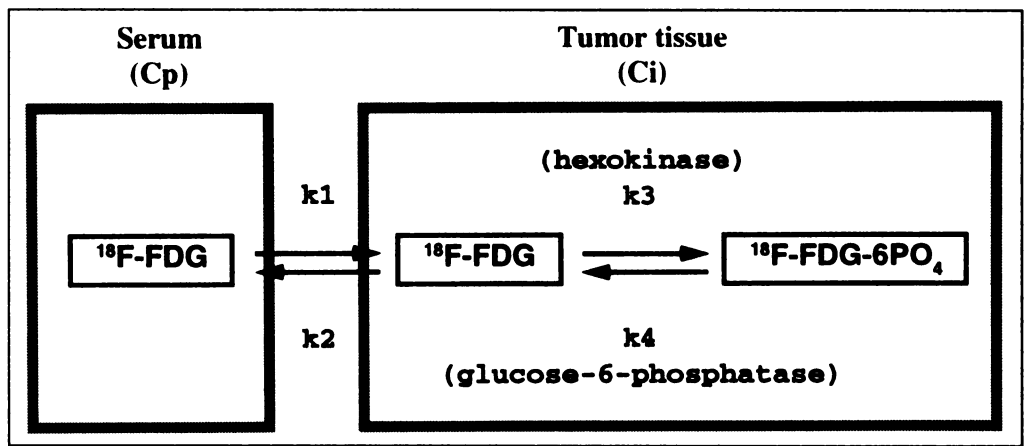
FIGURE 1. Compartment model of ^{18}F-FDG. k1–k4 = rate constants; Cp = changes in radioactivity of plasma; Ci = changes in radioactivity of tumor.

RESULTS

PET and SUV

All esophageal cancers showed marked accumulation of ^{18}F-FDG at 60 min after tracer injection (Fig. 2). In SUV, esophageal cancers had significantly higher values (6.99 ± 3.05, n = 48) than either benign tumors (0.86, n = 1) or normal control subjects (1.34 ± 0.37, n = 10). In malignancies, 47 of 48 patients had SUVs greater than 2.0, and all nonmalignant tissues had SUVs less than 2.0 (Fig. 3). It was possible to distinguish malignant tumors from benign lesions by using the cutoff value of 2.0 (accuracy rate 98.3%) (11,12).

Estimation of Glucose Metabolism and SUV

Since the radioactivity change of labeled FDG in tumors were considered to depend on rate constants, a ^{18}F-FDG dynamic study was performed on 11 patients with esophageal cancer to calculate the rate constants.

The k4 value (dephosphorylation by glucose-6-phosphatase), 0.008 ± 0.007/min, was significantly lower than the k3 value (phosphorylation by hexokinase), 0.143 ± 0.053/min, in esophageal cancer (Fig. 4).

Hexokinase activities from resected specimens were measured in 13 patients with esophageal cancer (5.01 ± 2.11 U/g
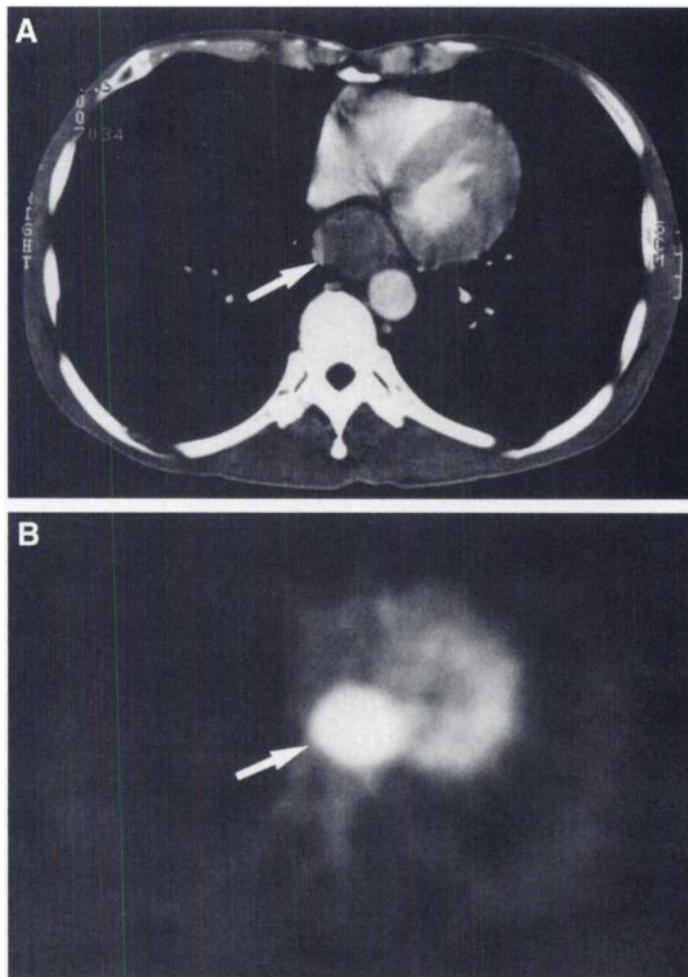
FIGURE 2. CT (A) and FDG PET (B) images of esophageal cancer. White arrow (B) shows a marked accumulation of ^{18}F-FDG at the same position identified on the CT image (A).
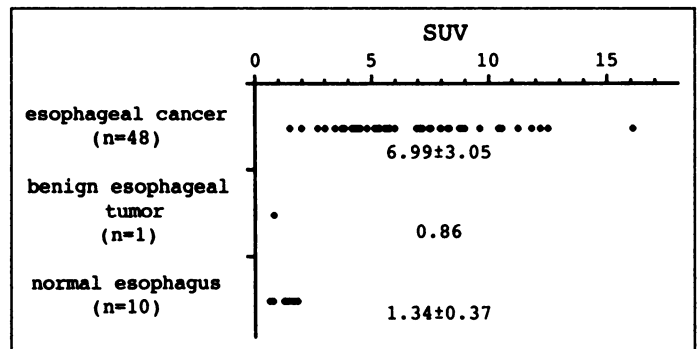
FIGURE 3. SUVs in esophageal cancers and other states. All esophageal cancers except one reveal SUVs of greater than 2.0 (mean ± s.d.; 6.99 ± 3.05). Ten normal control subjects and one patient with a benign esophageal tumor had SUVs < 2.0 (1.34 ± 0.37, 0.86).
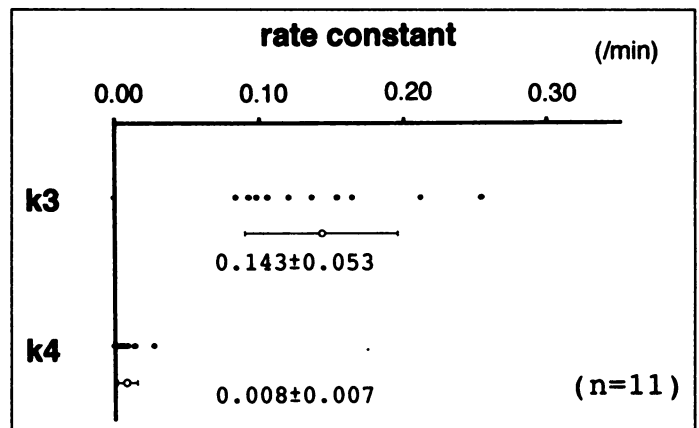
FIGURE 4. Values of rate constants k3 and k4 in 11 esophageal cancers. The k3 value (reflects the hexokinase activity) is definitely higher than the k4 value (reflects the glucose-6-pase activity). The k4 value can be neglected in esophageal cancers.
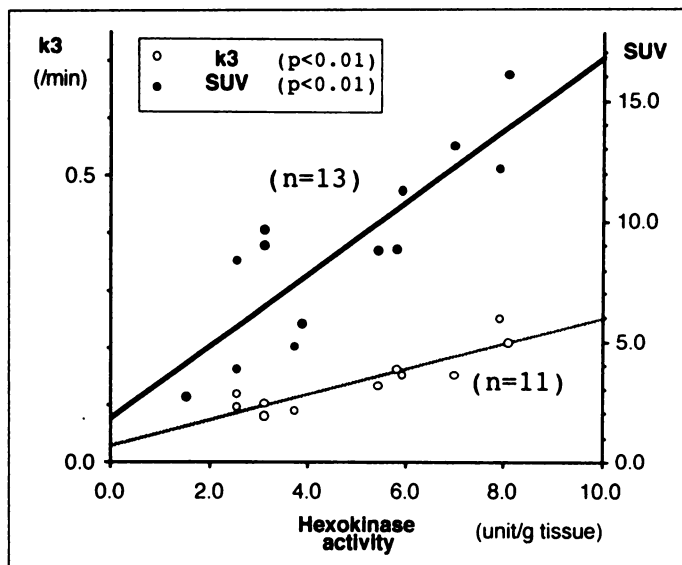
FIGURE 5. The relationship between hexokinase activity, k3 and SUV. Both k3 and SUV are well correlated with hexokinase activity in esophageal cancers.

tissue). Both the k3 value and SUV were well correlated with hexokinase activity of tumor (p < 0.001) (Fig. 5).

Clinical and Pathological Findings and SUV

Clinical and pathological findings of 48 resected patients are shown in Table 1 (*13,14*). The information in Table 1 can be summarized as follows:

1. Age: No statistical correlation between age and SUV were evident.
2. Location of the lesion: Lesions were located in the cervical esophagus in 4 patients (SUV = 5.90 ± 1.52), upper thoracic portion in 5 (6.39 ± 4.47), midthoracic portion in 29 (7.36 ± 3.19) and lower thoracic and abdominal esophagus in 10 (6.67 ± 2.47). No significant differences in SUV were evident.
3. Vertical extension: Length of tumors, as measured from resected specimens, ranged 3.5–23.0 cm (7.4 ± 3.5). No correlation between vertical extension and SUV were evident.
4. Histologic classification: The resected patients were divided into 5 groups by histological grading as follows: Group 1 = well differentiated (n = 11); Group 2 = moderately differentiated (n = 25); Group 3 = poorly differentiated (n = 8); Group 4 = undifferentiated (n = 2); and Group 5 = carcinosarcoma (n = 2). SUVs were 6.64 ± 3.14, 6.91 ± 2.57, 6.24 ± 2.45, 7.48 ± 6.70 and 12.50 ± 5.13, respectively. Carcinosarcoma revealed significantly high values compared to others (p < 0.05); however, no significant differences were evident between Groups 1–4.
5. Depth of invasion: The patients were divided into 4 groups by depth of invasion as follows: pT1 to submucosa (n = 4); pT2 to muscularis propria (n = 10); pT3 to adventitia (n = 31) and pT4 to adjacent structures (n = 3). SUVs were 6.81 ± 6.42, 7.06 ± 2.01, 7.12 ± 2.97 and 5.69 ± 1.98, respectively. No significant differences were evident between pT- pT4.
6. Lymph node metastasis: Absence of lymph node metastasis was revealed in 11 patients (pN0pM0), regional lymph node metastasis in 20 (pN1pM0) and distant metastasis in 17 (pM1LYM). SUVs were 6.93 ± 2.75, 7.15 ± 2.84 and 6.85 ± 3.61, respectively. No significant differences were evident between pN0pM0, pN1pM0 and pM1LYM.
7. pTNM classification: Through categorization by pTNM classification, 10 patients were classified as Stage IIA, 4 as Stage IIB, 17 as Stage III and 17 as Stage IV. SUVs were 7.15 ± 2.80, 5.54 ± 3.33, 7.39 ± 2.66 and 6.85 ± 3.61, respectively. No significant differences were evident between Stages IIA- IV.

Prediction of Prognosis and SUV

The radically resected patients were divided into two groups: Group A and Group B, according to SUVs. All 48 patients underwent radical resection, thereby excluding absolute noncurative surgeries. Group A includes 25 patients with SUVs less than 7.0 (the approximate average of SUVs), and Group B includes 23 patients with SUVs greater than 7.0. Table 2 shows the SUV and pTNM classification of these two groups. No difference in each factor was observed in each group. Figure 6 shows the cumulative survival rate without recurrence after surgery in each group. The survival rate was significantly high in Group A (p < 0.05). Furthermore, in patients with lymph node metastasis (Fig. 7) and Stages III and IV classification (Fig. 8), a high SUV tended to result in a poor prognosis in comparison to low SUVs (p < 0.01, p < 0.05).

DISCUSSION

In this study, ^{18}F-FDG was used as a tracer for glucose metabolism and PET was performed to examine glucose metabolism of esophageal cancer. Glucose metabolism increases in malignant tumors (*15*), and in the glycolytic pathway, hexokinase activity correlates with tumor proliferative activity. Fluorine-18-FDG is phosphorylated by hexokinase within the cells and accumulates intracellularly as ^{18}F-FDG-6-PO$_4$, since it is not a substrate of phosphohexose isomerase (the enzyme involved in the next step of the glycolytic pathway). The measurement of glucose metabolism using ^{18}F-FDG is reported as a metabolic model for the brain by Phelps et al. (*9*) based on Sokoloff's model (*16*). In this study, since the k3 value was well correlated with the measured hexokinase activity, this model seemes to be reliable for the analysis of esophageal cancers.

SUV is one of the most convenient and common indices of tracer uptake in PET studies. It is easily calculable from radioactivities of tumors, injected dose of ^{18}F-FDG, body weight and physical decay (*8*). It had been used as an index of ^{18}F-FDG uptake in previous reports, but there are currently no reports examining the correlation between the rate constant and SUVs of esophageal cancer. Our dynamic study revealed that the k4 value of esophageal cancer was significantly lower than k3. This result is consistent with a previous report in which glucose-6-phosphatase presents specifically in the liver and kidneys but not in tumors and other tissues (*17,18*). Given that ^{18}F-FDG uptake by tumor cells as a function of the enzyme ratio of hexokinase to glucose-6-phosphatase, ^{18}F-FDG uptake in esophageal cancer may depend solely on hexokinase activity, since glucose-6-phosphatase activity tends to be negligible. The reliability of SUV as a marker for observing hexokinase activity in esophageal cancer was confirmed by evidence of correlation of the SUV with hexokinase activity and the k3 value. Focally inflammatory lesions are known to show high ^{18}F-FDG uptake at times due to increased metabolic activity of leukocytes and other inflammatory cells, however, since no patient in this study presented with esophagobronchial fistula or other infectious lesions, SUV could be used as a convenient index to assess glucose metabolism in esophageal cancer.

TABLE 1
Clinical and Pathological Findings and SUV (Resected 50 Cases)

Patient no.	Age (yr)	Sex	SUV	Location	Length (cm)	Histologic classification	pT	pN	pM	TNM stage
1	72	M	1.53	Iu	5.5	Moderate	1	1	0	IIB
2	46	M	2.04	.E	7.0	Well	3	0	0	IIA
3	64	M	2.74	Im	4.0	Undetermined	3	1	1	IV
4	57	M	3.05	Iu	4.0	Well	3	1	1	IV
5	72	M	3.47	Im	9.0	Moderate	3	1	0	III
6	76	M	3.75	E	8.4	Poor	3	1	0	III
7	58	M	3.90	Im	8.0	Poor	3	1	0	III
8	61	M	4.18	Im	4.0	Poor	1	1	0	IIB
9	53	F	4.28	Ce	9.0	Well	4	1	1	IV
10	72	F	4.35	Im	3.5	Well	3	0	1	IV
11	62	M	4.47	Im	9.0	Moderate	2	1	1	IV
12	71	M	4.55	Im	7.0	Well	3	0	0	IIA
13	63	M	4.83	Im	9.0	Moderate	4	0	0	III
14	57	M	5.16	Im	3.7	Moderate	2	1	1	IV
15	69	M	5.16	Im	10.0	Moderate	3	1	1	IV
16	58	M	5.30	E	5.5	Moderate	3	1	0	III
17	54	F	5.39	Im	5.5	Moderate	1	0	1	IV
18	70	M	5.63	Ce	6.0	Moderate	2	0	0	IIA
19	66	M	5.64	E	4.1	Moderate	2	0	1	IV
20	63	M	5.73	Ce	4.0	Poor	2	0	1	IV
21	51	M	5.74	Im	8.0	Moderate	3	1	0	III
22	61	M	5.78	Im	5.0	Moderate	3	0	0	IIA
23	51	M	5.82	Iu	23.0	Poor	3	1	1	IV
24	51	M	6.04	Im	5.6	Moderate	3	1	0	III
25	67	M	6.97	E	11.5	Moderate	3	1	1	IV
26	56	M	7.12	Im	5.5	Moderate	3	0	0	IIA
27	70	M	7.23	E	7.0	Moderate	3	1	0	III
28	44	M	7.51	Im	5.8	Well	3	0	0	IIA
29	46	M	7.59	Im	6.0	Poor	2	1	0	IIB
30	50	F	7.95	Ce	5.0	Moderate	4	1	0	III
31	59	M	7.99	Im	13.0	Well	2	1	1	IV
32	68	M	8.29	Im	7.0	Moderate	3	1	0	III
33	59	M	8.34	Im	6.0	Moderate	3	1	0	III
34	56	M	8.39	E	10.5	Poor	3	0	0	IIA
35	69	F	8.82	Im	7.0	Moderate	3	1	0	III
36	62	M	8.87	E	6.5	Carcinosarcoma	2	1	0	IIB
37	52	M	8.87	Im	8.0	Well	2	0	0	IIA
38	65	M	8.88	E	8.0	Well	3	1	0	III
39	76	M	9.05	Iu	7.0	Moderate	3	1	0	III
40	63	M	9.66	E	7.0	Well	3	0	0	IIA
41	72	M	10.47	Im	10.2	Moderate	3	1	0	III
42	51	M	10.50	Im	4.5	Moderate	3	1	1	IV
43	55	M	10.60	Im	12.8	Poor	2	1	1	IV
44	58	M	11.31	Im	4.5	Moderate	3	1	0	III
45	62	M	11.89	Im	5.0	Well	3	0	0	IIA
46	69	M	12.22	Im	16.0	Undetermined	3	1	0	III
47	69	M	12.52	Iu	5.0	Moderate	3	1	1	IV
48	72	M	16.13	Im	8.0	Carcinosarcoma	1	1	1	IV

Ce = cervical esophagus; Iu and Im = upper and middle intrathoracic esophagus; E = lower esophagus.

Since patients with esophageal cancers presented with significantly higher values than those with benign tumors or normal control subjects, malignant tumors can be distinguished from benign lesions by referring to the SUV cutoff value of 2.0 (accuracy rate 96.7%) (11). Clinically, ^{18}F-FDG PET should be used to assess postoperative esophageal cancer, because it can define early recurrence from miscellaneous mass lesions. Furthermore, recent studies have assessed the use of PET (espe-

TABLE 2
SUV and pTNM Classification in Groups A and B

Group	SUV classification	Primary tumor				Regional lymph nodes		Distant metastasis		pTNM classification			
		pT1	pT2	pT3	pT4	pN0	pN1	pM0	pM1	IIA	IIB	III	IV
A	SUV <7.0 (n = 25)	3	5	15	2	9	16	13	12	4	2	7	12
B	SUV ≥7.0 (n = 23)	1	5	16	1	6	17	18	5	6	2	10	5

cially whole-body PET) in preoperative staging of malignant tumors (*19*).

SUV may also be a useful diagnostic index to distinguish
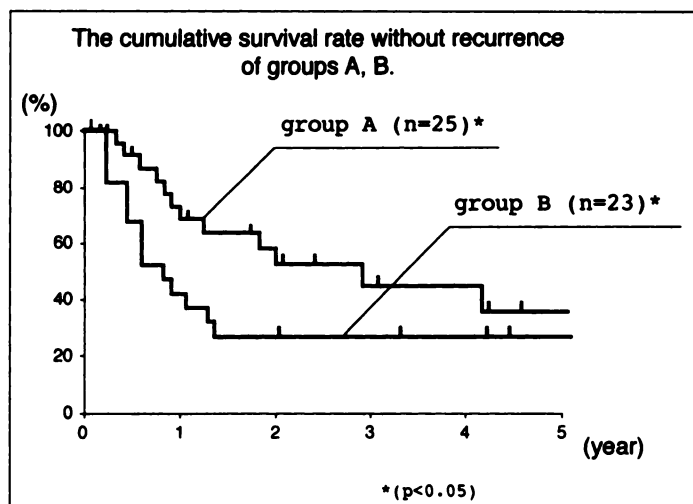

FIGURE 6. The cumulative survival rate without recurrence after surgery for Groups A and B. Prognosis is favorable for Group A.
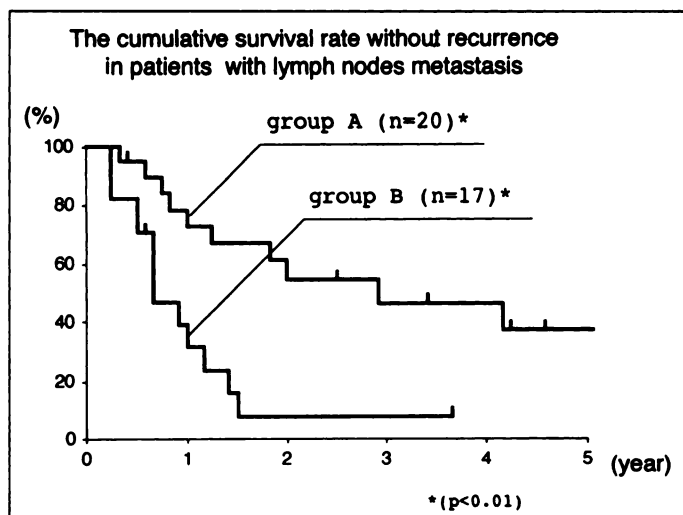

FIGURE 7. The cumulative survival rate without recurrence in patients with lymph node metastasis. Relapse was observed in Group B within 2 yr except for one patient.
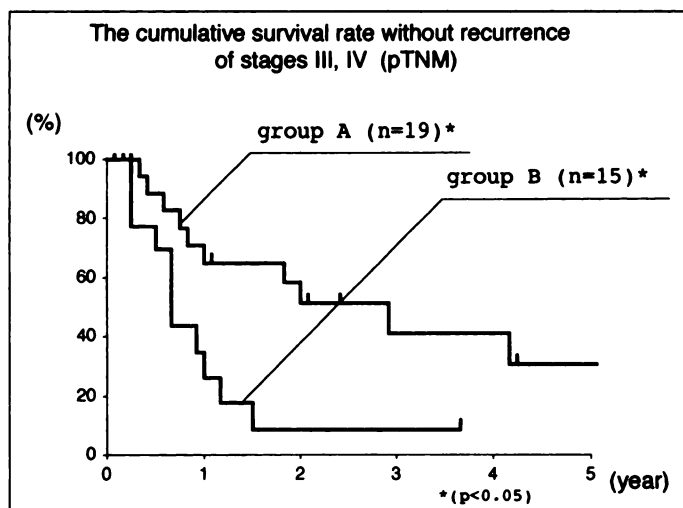

FIGURE 8. The cumulative survival rate without recurrence for Stages III and IV (pTNM). In Group B, early recurrence appeared.

malignant tumors from benign lesions and elucidate prognosis after surgery. In this study, patients with higher SUVs had poor prognoses in comparison to those with low SUVs. Two possible explanations for this tendency exist. First, SUV may be representing the measurement of growth rate of residual cancer cells. In previous publications, glucose utilization was reported to be higher in rapidly growing tumors as compared to less aggressive low-grade neoplasms (*20–22*). Actually, recurrent cases with higher values of preoperative SUV had shorter latent periods after operation than those with lower values. Accordingly, frequent follow-ups are vital in cases with high SUV value. Second, SUV may be assessing tumor viability (*23*). Variable prognosis observed in patients having similar radiological and pathological findings. It may be caused by the viability of cancer cells. In our previous report, DNA ploidy patterns were actually well correlated with ^{18}F-FDG uptake (*24*). In accordance, high SUV levels may be indicative of preoperative adjuvant therapy.

Since SUV is easily obtained by a static study, repetitive analyses are possible. Accordingly, it is a useful index for repetitive assessments of treatment effect (*25*) and postoperative follow-up. The subjects of this study were restricted by tumor size due to limited resolution of the PET scanner, however, recent technical advancements have made analysis of smaller esophageal cancers possible.

CONCLUSION

Fluorine-18-FDG PET was executed to elucidate glucose metabolism in esophageal cancer. Evaluation of ^{18}F-FDG uptake was manifested by SUV. SUV of patients with esophageal cancer is: (a) well correlated with hexokinase activity of the resected specimen; (b) useful for distinguishing malignant tumors from benign lesions by referring to the cutoff value of 2.0; and (c) regarded as a useful index for predicting prognosis before surgery. Consequently, SUV is a vital index for clinical assessment of esophageal cancer.

REFERENCES

1. Sharma RM, Sharma C, Donnelly AJ, et al. Glucose-ATP phospho-transferases during hepatocarcinogenesis. *Cancer Res* 1965;25:196–199.
2. Knox WE, Jamdar SC, Davis PA, et al. Hexokinase, differentiation and growth rates of transplanted rat tumors. *Cancer Res* 1970;30:2240–2244.
3. Di Chiro G. Positron emission tomography using [18F]fluorodeoxyglucose in brain tumors: a powerful diagnostic and prognostic tool. *Invest Radiol* 1987;22:360–371.
4. Yonekura Y, Benua RS, Brill AB, et al. Increased accumulation of 2-deoxy-2[18F]fluoro-D-glucose in liver metastasis from colon cancer. *J Nucl Med* 1982;23:1133–1137.
5. Kubota K, Matsuzawa T, Fujiwara T, et al. Differential diagnosis of lung tumor with positron emission tomography: a prospective study. *J Nucl Med* 1990;31:1927–1932.
6. Okazumi S, Isono K, Enomoto K, et al. Evaluation of liver tumors using fluorine-18-fluorodeoxyglucose PET: characterization of tumor and assessment of effect of treatment. *J Nucl Med* 1992;33:333–339.
7. Yasuda S, Raja S, Hubner KF. Application of whole-body positron emission tomography in the imaging of esophageal cancer: report of a case. *Surg Today* 1995;25:261–264.
8. Woodard HQ, Bigler RE, Freed B, et al. Expression of tissue isotope distribution. *J Nucl Med* 1975;16:958–959.
9. Phelps ME, Huang SC, Huffman EJ, et al. Tomographic measurement of local cerebral glucose metabolic rate in humans with [18F]2-fluoro-2-deoxy-D-glucose: validation of method. *Ann Neurol* 1979;6:371–388.
10. Monakhov NK, Neistadt EL, Shavlovskii MM, et al. Physicochemical properties and isoenzyme composition of hexokinase from normal and malignant human tissues. *J Natl Cancer Inst* 1978;61:27–34.
11. Fukunaga T, Enomoto K, Okazumi S, et al. Evaluation of gastro-enterological disease by using ^{18}F-FDG-PET: differential diagnosis of malignancy from benignity. *Jpn J Nucl Med* 1992;29:687–690.
12. Yoshioka T, Takahashi H, Oikawa H, Kanemaru R. Experimental study on the effectiveness of PET tumor images for cancer diagnosis. *Jpn J Cancer Chemother* 1994;21:369–373.
13. Hermanek P, Sobin LH. *UICC: TNM classification of malignant tumours,* 4th revised ed. Berlin Heidelberg: Springer-Verlag; 1987.
14. Japanese Society for Esophageal Disease. *Guidelines for the clinical and pathologic studies on carcinoma of esophagus,* 8th ed. Tokyo: Kanehara; 1992.
15. Warburg O. On the origin of cancer cells. *Science* 1956;123:309–314.
16. Sokoloff L, Reivich M, Kennedy C, et al. The [14C]deoxyglucose method for the

measurement of local cerebral glucose utilization: theory, procedure, and normal values in the conscious and anesthetized albino rat. *J Neurochem* 1977;28:897–916.

17. Weber G, Cantero A. Glucose-6-phosphatase activity in normal, precancerous and neoplastic tissues. *Cancer Res* 1955;15:105–108.

18. Gallagher BM, Fowler JS, Gutterson NI, MacGregor RR, Wan CN, Wolf AP. Metabolic trapping as a principle of radiopharmaceutical design: some factors responsible for the biodistribution of [¹⁸F]2-deoxy-2-fluoro-D-glucose. *J Nucl Med* 1978;19:1154–1161.

19. Flanagan FL, Dehdashti F, Siegel BA, et al. Staging of esophageal cancer with ¹⁸F-fluorodeoxyglucose positron emission tomography. *Am J Roentgenol* 1997;168: 417–424.

20. Weber G. In: *The molecular correlation concept: studies on the metabolic pattern of hepatomas.* Tokyo: Maruzen Co.; 1966: 151–178.

21. Adler LP, Blair HF, Williams RP, et al. Grading liposarcomas with PET using [¹⁸F]FDG. *J Compt Assist Tomogr* 1990;14:960–962.

22. Duhaylongsod FG, Lowe VJ, Patz EF, Vaughn AL, Coleman RE, Wolfe WG. Lung tumor growth correlates with glucose metabolism measured by fluorine-18-fluorodeoxyglucose positron emission tomography. *Ann Thorac Surg* 1995;60:1348–1352.

23. Di Chiro G, Hatazawa J, Katz DA, et al. Glucose utilization by intracranial meningiomas as an index of tumor aggressivity and probability of recurrence: a PET study. *Radiology* 1987;164:521–526.

24. Fukunaga T, Enomoto K, Okazumi S, et al. Analysis of glucose metabolism in patients with esophageal cancer by PET: estimation of hexokinase activity in the tumor and usefulness for clinical assessment using ¹⁸F-fluorodeoxyglucose. *J Jpn Surg Soc* 1994;95:317–325.

25. Ichiya Y, Kuwabara Y, Otsuka M, et al. Assessment of response to cancer therapy using fluorine-18-fluorodeoxyglucose and positron emission tomography. *J Nucl Med* 1991;32:1655–1660.

Iodine-131-MIBG Scintigraphy in Adults: Interpretation Revisited?

V. Roelants, C. Goulios, C. Beckers and F. Jamar

Center of Nuclear Medicine, University of Louvain Medical School, Brussels, Belgium

Iodine-131-metaiodobenzylguanidine (MIBG) scintigraphy is a reliable method used to diagnose pheochromocytoma. Although the adrenal medulla usually is not visualized, faint uptake can be observed in 16% of the patients 48–72 hr after injection of 18.5–37 MBq ¹³¹I-MIBG. We recently observed an increase in the frequency of visualization of the adrenal medulla in patients injected with 74 MBq ¹³¹I-MIBG. Therefore, we retrospectively evaluated the pattern of uptake and potential changes between 1984 and 1994. **Methods:** Scintigraphic data from 103 patients referred for suspected pheochromocytoma were reviewed randomly. Data from 19 patients with medullary thyroid carcinoma were analyzed separately. Patients were injected with 74 MBq ¹³¹I-MIBG and imaged at 24 hr postinjection, 48 hr postinjection, or both. Adrenal uptake was scored visually as 0 (no visible uptake) and 1 (uptake just visible) to 4 (most intense activity in the picture). Semiquantitative indicies were evaluated for discriminating between normal adrenal medullae and pheochromocytomas. Twenty-seven pheochromocytomas were surgically proven in 25 patients. **Results:** A visual score ≥3 was noted in 81% and 90% of the pheochromocytomas at 24 hr and 48 hr postinjection, respectively. From 1984 to 1988, 16% and 31% of adrenal medullae were seen at 24 and 48 hr postinjection, respectively, whereas from 1989 to 1994, 56% and 73% were visualized at 24 and 48 hr postinjection, respectively. Before 1989, the best cutoff criterion to identify a pheochromocytoma, determined from receiver operating characteristic curve analysis, was a score ≥1 at 24 hr and ≥3 at 48 hr postinjection, with a sensitivity and specificity of 92% and 84% at 24 hr and 92% and 99% at 48 hr postinjection. From 1989, the best cutoff was a score ≥3 at both imaging sessions, with a sensitivity and specificity of 82% and 100% at 24 hr and 100% and 97% at 48 hr postinjection. Among the semiquantitative indicies, the adrenal-to-liver and adrenal-to-heart ratios were the best discriminators between normal and pathological adrenals. They were, however, of little use because of the overlap between normal adrenal medullae and pheochromocytomas. **Conclusion:** The high rate of visualization of the normal adrenal medulla in this study was related to the larger-than-usual injected dose (74 MBq). Over recent years, however, this rate has been increasing, possibly because of the increased specific activity of ¹³¹I-MIBG. Adequate interpretation should take into account that a faint or definite uptake may be visible

in more than 50% of normal adrenal medullae.

Although rare, pheochromocytoma is a potentially life-threatening tumor that usually can be managed with minimal morbidity provided that it is diagnosed early (*1*). Since its introduction in 1980, metaiodobenzylguanidine (MIBG) labeled with ¹³¹I has proven to be a safe, noninvasive and efficient localization procedure. This is particularly true for tumors arising from extra-adrenal sites or exhibiting malignant metastatic disease and for postoperative tumor recurrence (*2–7*).

MIBG is an analog of the endogenous neurotransmitter norepinephrine, and two mechanisms of uptake have been described. The first is an energy- and sodium-dependent specific uptake mechanism (known as Type I); in addition, there is some degree of nonspecific diffusion (known as Type II). After entering neuroendocrine cells, MIBG is concentrated in the intracellular hormone storage vesicles by an energy-dependent, tetrebenazine-sensitive process similar to the cell membrane specific uptake mechanism (*8*). Uptake can be found in a variety of normal tissues, such as the adrenals, and the sympathetic innervation of the salivary glands and myocardium. Consistent with the neuroadrenergic uptake mechanism, there is a good correlation between the uptake of radioactivity and the amount of neurosecretory granules (*9*). The normal distribution of this agent was first described in detail by Nakajo et al. (*10*) in 1983. They found that, after injection of 18.5 MBq, normal adrenal medullae were observed only in 2% of patients at 24 hr and in 16% of patients at 48 hr postinjection, whereas pheochromocytomas had an intense focal area of uptake between 24 and 72 hr postinjection. Other researchers (*3, 4*) found that the adrenal medulla usually was not depicted using this dosage, whereas uptake could be delineated more frequently with higher doses.

Examining the ¹³¹I-MIBG distribution pattern over recent years, we had the impression that the adrenal medulla was more often visualized, although the prevalence of pheochromocytoma was stable (i.e., 2–3/yr) and the injected radioactivity